



Comparative transcriptome analysis provides insights into the molecular mechanism of the anti-nematode role of *Arachis hypogaea* (Fabales: Fabaceae) against *Meloidogyne incognita* (Tylenchida: Heteroderidae)

XUEJIN YANG^{1,2,*}; YUANYUAN ZHOU^{1,*}; XINYI PENG¹; XIAOHONG FU¹; JIANQING MA¹; JIANFENG LIU^{1,*}; DANDAN CAO^{1,2,*}

¹ College of Life Science, Institute of Life Science and Green Development, Hebei University, Baoding, 071002, China

² Hebei Innovation Center for Bioengineering and Biotechnology, Hebei University, Baoding, 071002, China

Key words: *Arachis hypogaea*, *Meloidogyne incognita*, Transcriptome data, *AhHPT* gene

Abstract: Background: Plant root-knot nematode (RKN) disease is a serious threat to agricultural production across the world. *Meloidogyne incognita* is the most prominent pathogen to the vegetables and cash crops cultivated. *Arachis hypogaea* can effectively inhibit *M. incognita*, but the underlying defense mechanism is still unclear. **Methods:** In our study, the chemotaxis and infestation of the second-stage juveniles (J2s) of *M. incognita* to *A. hypogaea* root tips were observed by the Pluronic F-127 system and stained with sodium hypochlorite acid fuchsin, respectively. The transcriptome data of *A. hypogaea* roots with non-infected or infected by J2s were analyzed. **Results:** The J2s could approach and infect inside of *A. hypogaea* root tips, and the chemotactic migration rate and infestation rate were 20.72% and 22.50%, respectively. Differential gene expression and pathway enrichment analyses revealed ubiquinone and other terpenoid-quinone biosynthesis pathway, plant hormone signal transduction pathway, and phenylpropanoid biosynthesis pathway in *A. hypogaea* roots responded to the infestation of *M. incognita*. Furthermore, the *AhHPT* gene, encoding homogentisate phytyltransferase, was considered to be an ideal candidate gene due to its higher expression based on the transcriptome data and quantitative real-time PCR analysis. **Conclusion:** Therefore, the key gene *AhHPT* might be involved in the *A. hypogaea* against *M. incognita*. These findings lay a foundation for revealing the molecular mechanism of *A. hypogaea* resistance to *M. incognita* and also provide a prerequisite for further gene function verification, aiming at RKN-resistant molecular breeding.

Introduction

Root-knot nematode (RKN; *Meloidogyne* spp.) is an important sedentary plant endoparasitic pathogenic nematode with a wide range of hosts (Aiouf *et al.*, 2022; Nishat *et al.*, 2022), which can infect more than 5,500 kinds of plants such as food crops and vegetables (Jaouannet *et al.*, 2012). Global agricultural losses caused by RKN are estimated at \$157 billion annually (Abad *et al.*, 2008; Eldeeb *et al.*, 2022). The second stage juveniles (J2s) of RKN search for the root system of the host plant by receiving chemical signals (Reynolds *et al.*, 2015), further invade meristem from

the plant root tips, and subsequently travel intracellularly along the vascular cylinder and remodel the parenchymal cells into giant cells as their feeding sites. The physiology and metabolism of plants will be seriously affected once they are infected by RKN (Davis *et al.*, 2000). For example, the aboveground part of plants is short, and the leaf color is abnormally yellow with deciduous and withered, which has a significant inhibitory effect on the growth of plant seedlings (Oka *et al.*, 2015; Elnahal *et al.*, 2022). With global climate change, reform of planting systems, and the rapid development of large-scale, mechanized, and high-value agriculture, RKN have gradually become one of the most serious pathogenic nematodes affecting agriculture cultivation (Jones *et al.*, 2013). *Meloidogyne incognita*, *M. hapla*, *M. javanica*, and *M. arenaria* are the main RKN species, among which *M. incognita* is recognized as the most prominent pathogen (Moens *et al.*, 2009). Therefore, the safe and effective prevention to control *M. incognita* has

*Address correspondence to: Jianfeng Liu, jianfengliu@hbu.edu.cn; Dandan Cao, dandancao@hbu.edu.cn

#These authors contributed equally to this work

Received: 27 February 2023; Accepted: 01 June 2023;

Published: 28 September 2023



become the bottleneck problem of high-quality and -yield for agricultural production and double reduction of chemical fertilizers and pesticides (Ali *et al.*, 2022; EI-Ashry *et al.*, 2023).

Arachis hypogaea L. is the main oil crop belonging to the family Leguminosae, subfamily Papilionatae, and is economically important as a source of proteins, minerals, and vitamins. It is widely grown in the semi-arid tropics and plays a role in the world agricultural economy. From the 1990s, the global planting area for *A. hypogaea* gradually increased, with a global production of about 48 million tons in 2019 (Çiftçi and Suna, 2022). However, in North America, South America, Africa, Asia, and Europe, *A. hypogaea* production areas have been reported to be mainly infested with three pathogens, namely, *M. arenaria*, *M. javanica*, and *M. hapla*, resulting in considerable yield loss (Dong *et al.*, 2008). Previous studies showed that only *M. arenaria* was isolated from the root-knot of the *A. hypogaea* root system grown in soils containing *M. incognita* and *M. arenaria* (Johnson *et al.*, 2000). To verify the reproduction of *M. incognita* on *A. hypogaea* plants, 2000 eggs of *M. incognita* were inoculated into *A. hypogaea* roots; however, no *M. incognita* could reproduce on *A. hypogaea* plants (Faske and Starr, 2009). In addition, the population density of *M. incognita* in soil was effectively reduced by continuous cropping of *A. hypogaea* (Johnson *et al.*, 1998). Compared with planting tomatoes, planting *A. hypogaea* could reduce the infestation rate of *M. incognita* by 70% (Belcher and Hussey, 1977). Several studies have proved that *A. hypogaea* is a non-host plant of *M. incognita* and has a certain inhibitory (or killing) effect on *M. incognita*.

The approach of screening and identifying resistance genes in non-host and high-resistant plant varieties is the key to successful molecular breeding for anti-RKN properties. The resistance genes *Mi-1*, *Mi-2*, *Mi-3*, *Mi-4*, *Mi-5*, *Mi-6*, *Mi-7*, *Mi-8*, *Mi-9*, and *Mi-HT* against *M. incognita* have been identified in tomato (El-Sappah *et al.*, 2019; Du *et al.*, 2020). When *Capsicum annuum* L. was infected by *M. incognita*, the expression level of the *CaRKNR* gene significantly increased, and silencing this gene by the virus-induced gene silencing system significantly reduced the resistance to *M. incognita* of pepper (Mao *et al.*, 2015). The *MIC* gene was also found to be closely related to the resistance of *M. incognita* in *Gossypium hirsutum* L. (Wubben *et al.*, 2008). At present, transcriptome analysis has been used to study the mechanism of plant and RKN interactions. Gene expression of soybean (*Glycine max*) infested with *M. incognita* for 12 days and 10 weeks revealed changes in expressions of genes involved in carbohydrate and cell wall metabolism, cell cycle control, and plant defense (Ibrahim *et al.*, 2011). Comparison of the transcriptome of *Polianthes tuberosa* uninfected and infected by *M. incognita* in the early, middle, and late periods revealed differential gene functions mainly in the pathways related to carbohydrate metabolism, signal transduction, and translation (Singh *et al.*, 2022). The screening of resistance genes, especially the obtaining of more accurate and effective resistance genes based on transcriptomics, has become the main strategy for plants to breed resistant-nematode varieties.

At present, the study of the interaction between *A. hypogaea* and *M. incognita* only focused on the inhibition phenomenon manifested in reducing the activity and the density population of *M. incognita*. The internal mechanism of *A. hypogaea*-*M. incognita* interaction is still poorly understood. The main hypothesis of our study is that *M. incognita* J2s can collect and infect the *A. hypogaea* root tips. *M. incognita* J2s infestation can cause differential expression of genes, which maybe play a key role in the interaction between *A. hypogaea* and *M. incognita*. Especially, the key gene *AhHPT* might be involved in *A. hypogaea* against *M. incognita*. Our findings will provide a strong background for identifying possible gene targets in *A. hypogaea* to develop broad resistance of plants to *M. incognita* by gene silencing technology or gene super-expression technology.

Materials and Methods

Experimental material

The initial sample of *M. incognita*, which was provided by the Academy of Agriculture and Forestry Sciences of Beijing, China, was propagated in living tomato plants in the laboratory incubator. The tomato variety was Qinshu Shanghai 908, provided by Xi'an Qinshu Agriculture Company Limited (China). Xiaobaisha (Fuhuasheng as female parent and Shitouqi as male parent), a widely cultivated *A. hypogaea* variety, was used as the experiment material. The study was conducted at the Agricultural Environmental Ecology Research Laboratory of Hebei Innovation Center for Bioengineering and Biotechnology of Hebei University, China (38°87' N, 115°51' E).

Nematodes collection and *Arachis hypogaea* cultivation

Tomato roots infected with *M. incognita* were selected, and the surface soil was removed by washing. The mature egg masses on the roots were picked with sterilized forceps under the stereomicroscope. The selected egg masses were thoroughly washed with 2% sodium hypochlorite solution for 3 min, and the remaining sodium hypochlorite solution was washed 3–4 times with sterile water. The washed egg masses were placed in a 500-mesh screen, placed in a Petri dish with sterile water, and incubated for 3–4 d in the dark constant temperature incubator at 27°C. The hatched J2s were collected.

A. hypogaea seeds (Cultivar Xiaobaisha) of the same size were soaked in 5% sodium hypochlorite solution for 15 min, washed 3–4 times with sterile water, placed in sterile Petri dishes containing sterile water for germination promotion at 27°C in the dark. After 3 d, each *A. hypogaea* was transplanted into 250 g sterilized soil (nutritive soil: vermiculite = 1:1 v/v) in a plastic pot of 11 cm in height and diameter and cultured in an intelligence artificial climate chamber until the *A. hypogaea* grew into two true leaves. The intelligence artificial climate chamber was set to two stages; the first stage was 16 h, 26°C, relative humidity 60%, light intensity 350 $\mu\text{mol}\cdot\text{m}^{-2}\cdot\text{s}^{-1}$, and the second stage was 8 h, 20°C, relative humidity 75%, light intensity 0 $\mu\text{mol}\cdot\text{m}^{-2}\cdot\text{s}^{-1}$.

Nematode treatment of excised Arachis hypogaea root tips

Twenty-three grams of Pluronic F-127 was added to a beaker containing 80 mL cold, sterile water and a magnetic stirring rod, stirred slowly at 4°C until dissolved. In the 6-well cell culture plate, 3 mL of 23% Pluronic F-127 and 10 µL suspension containing 100 J2s were added into each well. After mixing, a 1 cm of *A. hypogaea* root tip with similar shape and size was added into each well. 27°C in dark conditions after 3, 6, 9, 12, 18, 24, 30, 36, 48, 54 and 60 h, the stereomicroscope was used to observe the behavioral responses. The number of J2s in the range of 1 mm near the root tip of excised *A. hypogaea* was counted. At 30, 36, 42, 48, 54, 60, 66 and 72 h, the protocol of Byrd *et al.* (1983) was used to stain the nematodes in *A. hypogaea* root tips. Six replicates were set in each period, and the experiment was repeated three times.

Nematode treatment of potted Arachis hypogaea

The incubation of the J2s and the cultivation of *A. hypogaea* were the same as mentioned in the previous experiment. The *A. hypogaea* with strong and uniform growth were randomly divided into two groups. One group was inoculated with sterile water as the control group, the other group was inoculated with a suspension containing 2000 J2s per *A. hypogaea* plant. The amount of sterile water inoculated was consistent with the amount of suspension. The glass rod was used to dig two holes of 2 cm symmetrically, 1 cm away from the root of *A. hypogaea* as the inoculation site. The *A. hypogaea* roots in the two groups of 3, 9, and 15 d after treatment were selected and dyed according to the above staining method. Each treatment was repeated three times, and there were 18 samples marked as C3d_1, C3d_2, C3d_3, C9d_1, C9d_2, C9d_3, C15d_1, C15d_2, C15d_3, T3d_1, T3d_2, T3d_3, T9d_1, T9d_2, T9d_3, T15d_1, T15d_2 and T15d_3. All the collected *A. hypogaea* root samples were frozen in liquid nitrogen, stored at -80°C, and sent to Shanghai Majorbio Bio-pharm Technology Co., Ltd. (China). For transcriptome sequencing.

RNA extraction, purification, and detection

Total RNA was extracted from the *A. hypogaea* roots using TRIzol[®] Reagent according to the manufacturer's instructions, and genomic DNA was removed using DNase I (TaKara). RNA quality was determined by 2100 Bioanalyser (Agilent) and quantified using the ND-2000 (NanoDrop Technologies). The high-quality RNA samples (OD260/280 = 1.8 – 2.2, OD260/230 ≥ 2.0, RIN ≥ 6.5, 28S:18S ≥ 1.0, > 1 µg) were used to construct sequencing library.

Library preparation and Illumina Hiseq xten/Nova seq 6000 sequencing

RNA-seq transcriptome library was prepared following TruSeq[™] RNA sample preparation Kit from Illumina (San Diego, CA) using 1 µg of total RNA. Messenger RNA was isolated following to polyA selection method by oligo (dT) beads and fragmented by fragmentation buffer. Double-stranded cDNA was synthesized using a SuperScript double-stranded cDNA synthesis Kit (Invitrogen, CA) and random hexamer primers (Illumina). The synthesized cDNA was subjected to end-repair, phosphorylation, and 'A' base

addition according to Illumina's library construction protocol. Libraries were size-selected for cDNA target fragments of 300 bp on 2% Low Range Ultra Agarose followed by PCR amplified using Phusion DNA polymerase (NEB) for 15 PCR cycles. After quantification by TBS380, paired-end RNA-seq sequencing library was sequenced with the Illumina HiSeq xten/NovaSeq 6000 sequencer (2 × 150 bp read length).

Sequencing data quality control, comparison, and assembly

The raw paired-end reads were trimmed and quality controlled by SeqPrep (<https://github.com/jstjohn/SeqPrep>) and Sickle (<https://github.com/najoshi/sickle>) with default parameters. The clean reads were separately aligned to the reference genome with orientation mode using HISAT2 (<http://ccb.jhu.edu/software/hisat2>) software (Kim *et al.*, 2015). The mapped reads of each sample were assembled by StringTie (<https://ccb.jhu.edu/software/stringtie>) in a reference-based approach (Pertea *et al.*, 2015).

Analysis of differentially expressed genes (DEGs) and functional enrichment

To identify DEGs in different treatment groups and corresponding control groups, the expression level of each transcript was calculated according to the transcripts per million reads (TPM) method. RSEM (<http://deweylab.github.io/RSEM/>) software (Li and Dewey, 2011) was used to quantify gene abundances. DEGs analysis was performed using the DESeq2 (Love *et al.*, 2014) with $p \leq 0.05$ and $|\log_2FC| > 1$. The DEGs were screened by comparing all the genes expressed in *A. hypogaea* roots at different periods under nematode treatment. Functional-enrichment analysis through Gene Ontology (GO) and the Kyoto Encyclopedia of Genes and Genomes (KEGG) was performed to identify which DEGs were significantly enriched in GO terms and metabolic pathways at Bonferroni-corrected $p \leq 0.05$ and compared with all transcriptome data. GO functional enrichment, and KEGG pathway analysis were performed by Goatools (<https://github.com/tanghaibao/GOatools>) software and KOBAS (<http://kobas.cbi.pku.edu.cn>) software (Xie *et al.*, 2011).

Quantitative real-time PCR (qRT-PCR) analysis

Extraction of total RNA and removal of residual DNA from RNA were as described above. The first strand cDNA of RNA was synthesized by the UEIris II RT-PCR System for First-Strand cDNA Synthesis Kit (R2028, US Everbright[®] Inc., China). QRT-PCR was done using 2 × AueGreen qPCR Master Mix (S2008S, US Everbright[®] Inc., China). The thermal cycling program was as follows: 95°C for 5 min, followed by 45 cycles at 95°C for 15 s and 53°C for 60 s. *AhActin* was used as a reference gene to normalize target gene expression levels in the samples. The $2^{-\Delta\Delta CT}$ method was used to calculate the relative expression levels of stress-response genes. Primers were designed using Oligo 7 software, and the primer sequences are listed in Table 1.

Data statistical analysis

Origin 2022b software was used to analyze the chemotactic migration rate and infestation rate of J2s to excise *A.*

TABLE 1

The fluorescent quantitative primer

Gene ID	Forward primer sequence (5'-3')	Reverse primer sequence (5'-3')
<i>AhActin</i>	TTGGAATGGGTCAGAAGGATGC	AGTGGTGCCTCAGTAAGAAGC
arahy.Tifrunner.gnm1.ann1. W80L0M (<i>AhHPT</i>)	GACTCCAAACTTTAGCCGTA	TAATAGCAGCTCCATAAGCC

hypogaea root tips. Kruskal-Wallis test and one-way ANOVA were used to analyze the significance of the differences among different time periods. False discovery rate correction with Benjamini/Hochberg (BH) was adopted to conduct multiple test and corrections for *p*-value of DEGs analysis. Images were visualized by XT-10C stereomicroscope and Photoshop 2020 software.

Results

Aggregation of J2s near the excised *Arachis hypogaea* root tips
As shown in Fig. 1A, the J2s moved toward and aggregated near the excised *A. hypogaea* root tips. From 3 to 24 h, the number of the J2s near the root tip of *A. hypogaea* increased gradually. At 24 h, the chemotactic migration rate of J2s to the root tip of excised *A. hypogaea* was the highest, which was 20.72%. The chemotactic migration rate of the J2s to the excised *A. hypogaea* root tip decreased significantly to 10.22% at 30 h. The chemotactic migration rate of the J2s to the excised *A. hypogaea* root tip was 2.00% at 60 h (Fig. 1B).

Staining of the root tips isolated from *A. hypogaea* showed red J2s (Fig. 1C), indicating the invasion of J2s into the root of excised *A. hypogaea*, with an infestation rate of 22.50% at 66 h (Fig. 1D).

The Arachis hypogaea roots infected by J2s in the soil environment

The pot experiment was carried out considering that the activity of excised *A. hypogaea* root tips would affect the chemotaxis of J2s. Sodium hypochlorite acid fuchsin staining of *A. hypogaea* roots at 3, 9, and 15 d after J2s inoculation showed that J2s were observed in the meristem and elongation regions of *A. hypogaea* root crowns (Fig. 2).

Statistical analysis and quality evaluation of RNA-Seq

In this experiment, the genome of *A. hypogaea* (<https://data.legumeinfo.org/Arachis/hypogaea/annotations/Tifrunner.gnm1.ann1.CCJH/>) was used as a reference genome. The results of statistical analysis and comparison of sequencing data are shown in Table 2. The similarity analysis of

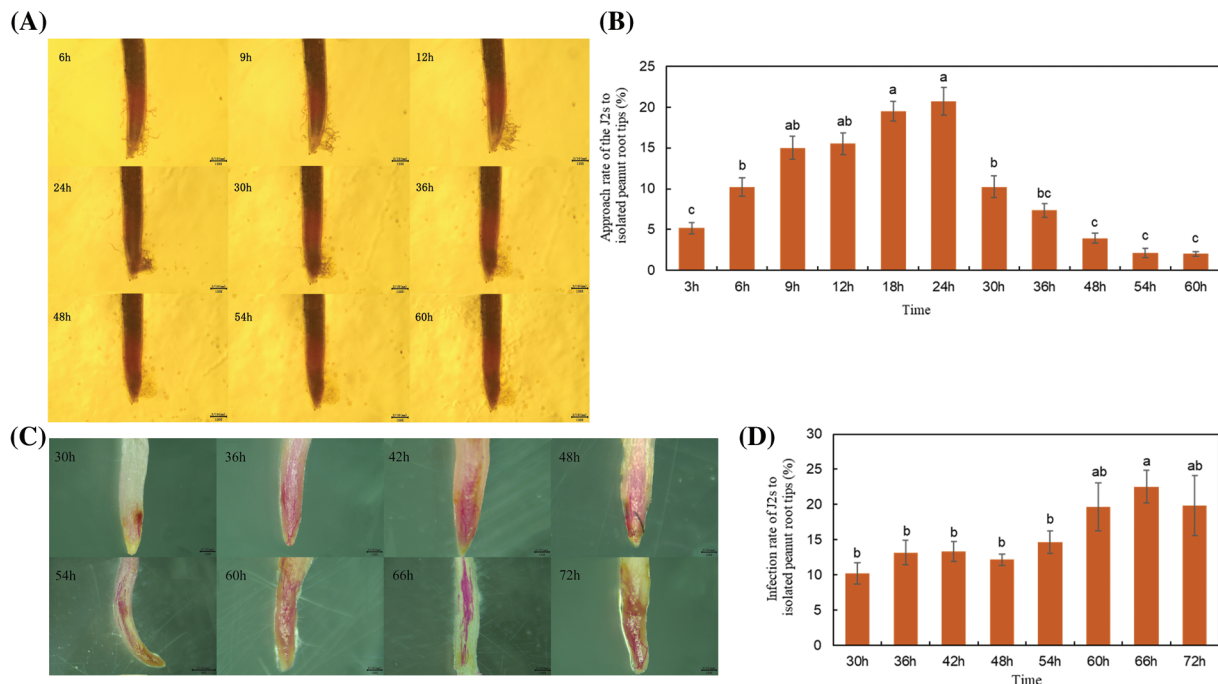


FIGURE 1. Assessment of chemotaxis and infestation of *Meloidogyne incognita* J2s to excised *Arachis hypogaea* root tips at different time points. (A) *M. incognita* J2s moved toward and aggregated near the excised *A. hypogaea* root tip at 6, 9, 12, 24, 30, 36, 48, 54, and 60 h. The scale is in the lower right corner. (B) Statistical representation of the chemotactic migration rate of the J2s to excised *A. hypogaea* root tip at different time points. (C) Staining of *M. incognita* J2s after entering the excised *A. hypogaea* root tip at different time points. The *M. incognita* that enters the peanut root is stained red. The scale is in the lower right corner. (D) The percentage of J2s invading the excised *A. hypogaea* root tip at different time points.

Note: Different bars in the bar charts are presented as means \pm standard error of the mean. The different lowercase letters above each bar chart indicated statistical significance at 0.05 level.



FIGURE 2. Pictures of J2s dyed after invading the *Arachis hypogaea* root tip at 3, 9, and 15 d in soil environment. Note: The black arrow points to the J2s, which were stained red.

sequences of 18 samples and the reference transcriptome database yielded a total of 135.6 G clean data. More than 6.73 G of clean data from each sample were obtained. The distribution of Q30 bases was 93.71%–94.57%, and the GC content was 45.45%–46.02%. The matching degree between the clean reads of each sample and the reference genome sequence was above 95%, with the highest matching rate of 96.54% and the lowest matching rate of 95.73%, indicating the accuracy and reliability of the sequencing.

Statistical analysis of differentially expressed genes

The results of principal component analysis (PCA) showed overlapping in the samples of C3d and T3d groups and the distance among the other groups was long (Fig. 3A), indicating that the gene expression difference between the C3d and T3d groups was not significant, while the difference between the other groups was significant. Three replicates within the same group were close to each other

and indicated consistent and uniform gene expression in the samples within the group. Comparison and analysis of the DEGs among the C3d vs. T3d, C9d vs. T9d, and C15d vs. T15d groups, a total of 3072 DEGs were obtained. The heat map of Fig. 3B showed the aggregation of DEGs. The gene expression of C3d was similar to that of T3d, with highly-expressed genes were mainly distributed in the upper parts of the heat map and low-expressed genes mainly distributed in the lower parts of the heat map. The genes with high expression of C9d were mainly distributed in the middle and upper parts of the heat map, while the genes with low expression were mainly distributed in the lower parts of the heat map. The high-expression genes in T9d were mainly distributed in the upper middle parts and the lower middle parts of the heat map. The high expression genes of C15d were mainly distributed in the lower parts of the heat map, and the low expression genes were mainly distributed in the upper parts of the heat map, while the

TABLE 2

Statistics of transcriptome sequencing

Sample	Raw reads	Clean reads	Q30 (%)	GC content (%)	Total mapped	Multiple mapped	Uniquely mapped
C3d_1	55,643,098	53,244,334	94.01	45.86	51,169,012 (96.1%)	9,183,627 (17.25%)	41,985,385 (78.85%)
C3d_2	52,584,958	50,882,190	94.35	45.89	48,887,460 (96.08%)	8,711,864 (17.12%)	40,175,596(78.96%)
C3d_3	51,349,076	49,190,854	93.86	45.85	47,266,701 (96.09%)	8,319,266 (16.91%)	38,947,435 (79.18%)
T3d_1	58,851,810	56,579,550	94.09	45.66	54,427,076 (96.2%)	10,010,663 (17.69%)	44,416,413 (78.5%)
T3d_2	64,738,158	62,040,356	94.27	45.8	59,704,294 (96.23%)	10,728,165 (17.29%)	48,976,129 (78.94%)
T3d_3	59,878,302	57,699,838	94.45	45.88	55,701,019 (96.54%)	10,090,132 (17.49%)	45,610,887 (79.05%)
C9d_1	48,672,858	46,928,914	93.87	45.98	44,992,507 (95.87%)	7,573,439 (16.14%)	37,419,068 (79.74%)
C9d_2	52,451,008	50,766,218	94.26	45.94	48,792,798 (96.11%)	8,398,906 (16.54%)	40,393,892 (79.57%)
C9d_3	51,344,694	49,663,494	94.05	46.02	47,545,120 (95.73%)	8,152,733 (16.42%)	39,392,387 (79.32%)
T9d_1	49,298,358	47,377,576	94.57	45.76	45,583,940 (96.21%)	8,131,801 (17.16%)	37,452,139 (79.05%)
T9d_2	51,937,752	50,008,500	93.71	45.9	47,988,583 (95.96%)	8,353,191 (16.7%)	39,635,392 (79.26%)
T9d_3	61,625,652	59,422,866	94.11	45.83	57,047,788 (96.0%)	10,027,933 (16.88%)	47,019,855 (79.13%)
C15d_1	51,152,166	49,451,734	94.35	45.73	47,478,878 (96.01%)	8,117,566 (16.42%)	39,361,312 (79.6%)
C15d_2	47,929,558	46,356,160	93.74	45.65	44,495,032 (95.99%)	7,660,856 (16.53%)	36,834,176 (79.46%)
C15d_3	50,922,158	49,094,736	94.32	45.45	47,213,316 (96.17%)	8,133,318 (16.57%)	39,079,998 (79.6%)
T15d_1	55,802,626	54,183,164	94.15	45.89	52,056,749 (96.08%)	9,364,540 (17.28%)	42,692,209 (78.79%)
T15d_2	52,264,386	50,632,680	93.95	45.8	48,651,881 (96.09%)	8,423,999 (16.64%)	40,227,882 (79.45%)
T15d_3	49,635,532	47,844,322	94.17	45.77	46,065,247 (96.28%)	7,982,427 (16.68%)	38,082,820 (79.6%)

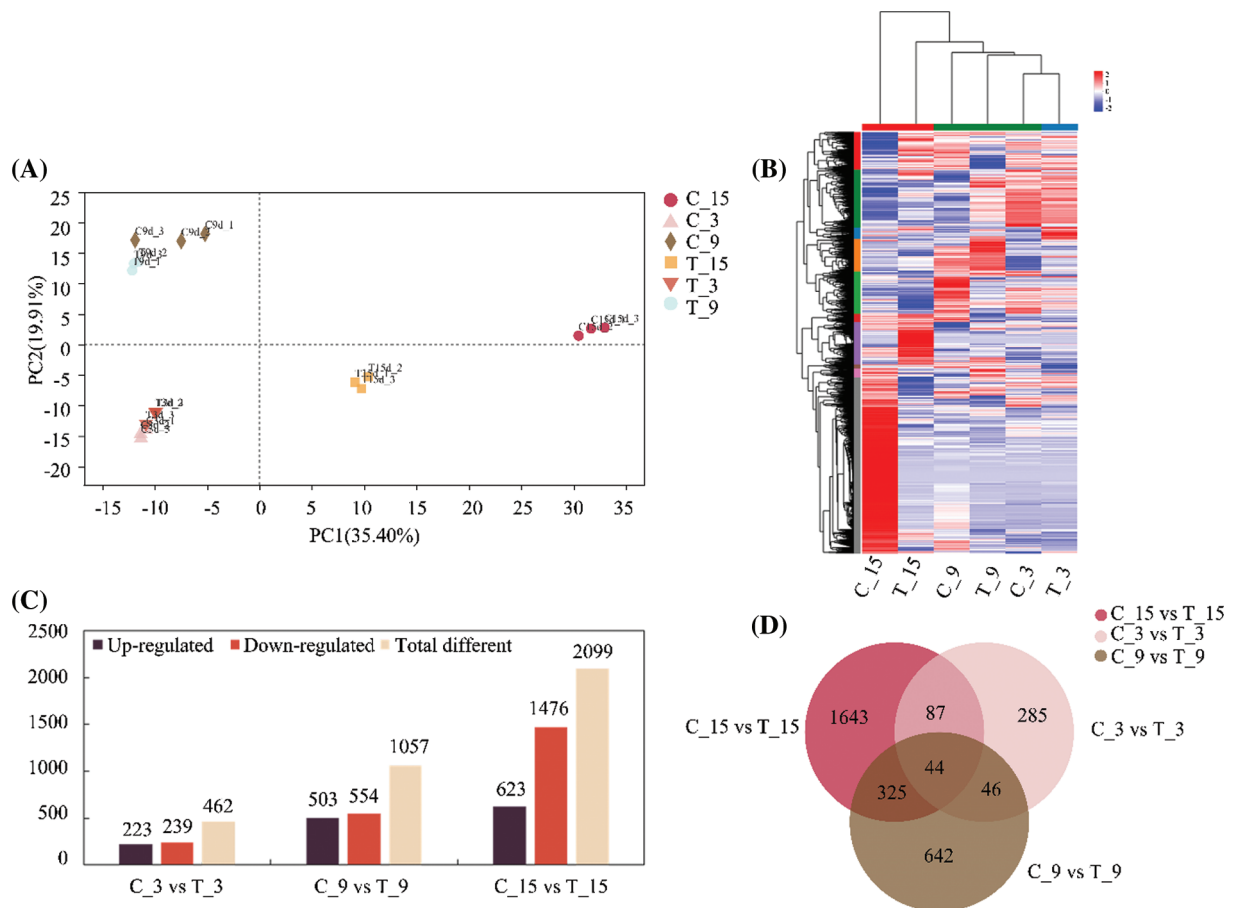


FIGURE 3. Analysis of differentially expressed genes (DEGs) in *Arachis hypogaea* roots responding to *Meloidogyne incognita* stress. (A) Principal component analysis of all samples. (B) Heatmap clustering of DEGs under different days of nematode treatment conducted using Hierarchical Clustering (HCL). The colors in the heatmap represent the normalized expression of the gene in each group. (C) Statistical presentation of the number of genes significantly regulated by nematode treatment on different days. (D) Venn diagram analysis of significant regulatory genes under different durations of nematode treatment.

high expression genes of T15d were mainly distributed in the middle and the upper parts of the heat map, and the low expression genes were mainly distributed in the lower parts of the heat map.

The DEGs of the three groups of nematode treatment groups and their respective control groups were statistically analyzed, and the results are shown in Fig. 3C. Statistical analysis showed that 462 DEGs were detected between C3d and T3d groups, of which 223 were up-regulated and 239 were down-regulated. Among C9d and T9d groups, 1057 DEGs were detected, including 503 genes with up-regulated expression and 554 genes with downregulated expression. The number of DEGs between C15d and T15d groups was 2099, including 623 with up-regulated expression and 1476 with down-regulated expression. The number of DEGs increased with the extension of nematode treatment time. There were 44 identical DEGs in the three treatment groups. The C3d vs. T3d, C9d vs. T9d, and C15d vs. T15d groups contained 285, 642, and 1643 unique DEGs, respectively. The C9d vs. T9d, and C15d vs. T15d groups had the largest number of genes with common differential expression, which was 369 (Fig. 3D).

Gene ontology functional enrichment analysis of differentially expressed genes in response to nematode treatment

GO function enrichment analysis was performed on the DEGs of the treatment groups and the control groups with various durations after inoculation. Statistical analysis of GO Terms, which considered significantly enriched DEGs ($p < 0.05$) in each group and ranked them in the top 30 of the enrichments, showed enrichment in GO terms related to plant defense response (Figs. 4A–4C). Twenty-two DEGs of C3d vs. T3d were significantly enriched in GO Term of plant defense response, of which 15 were up-regulated and 7 were down-regulated (Fig. 4D). In C9d vs. T9d, 43 DEGs were significantly enriched in GO terms of plant defense response, of which 24 were up-regulated, and 19 were down-regulated (Fig. 4E). There were 81 DEGs in C15d vs. T15d that were significantly enriched in the plant defense response GO Term, of which 24 were up-regulated, and 57 were down-regulated (Fig. 4F). The two genes with their IDs *arahy.Tifrunner.gnm1.ann1.NH8LJ7* and *arahy.Tifrunner.gnm1.ann1.VFVG10*, respectively, were present in the GO term of the plant defense response enriched by DEGs in the C3d vs. T3d, C9d vs. T9d, and C15d vs. T15d. The gene

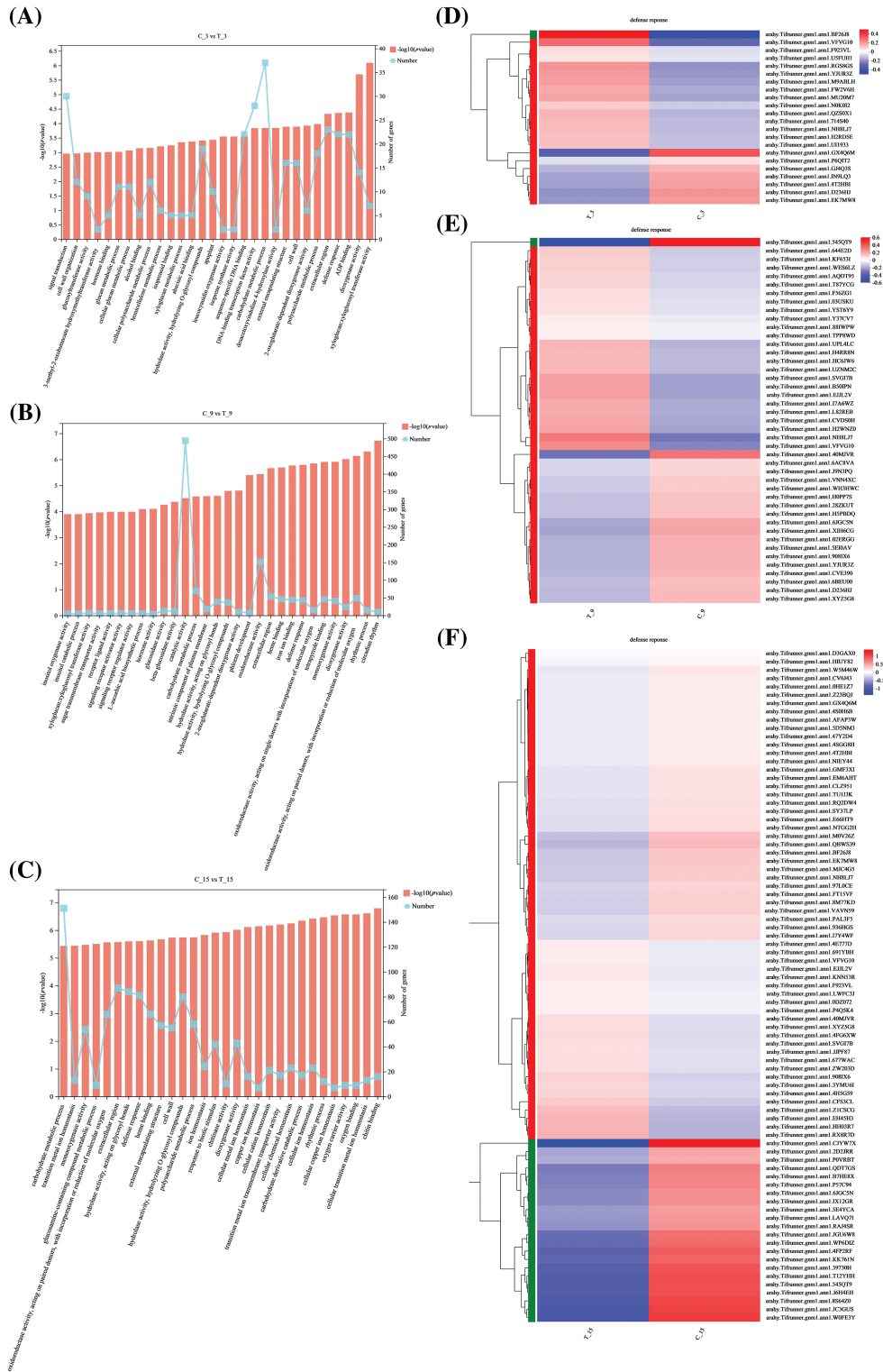


FIGURE 4. Gene Ontology (GO) enrichment results and heat map clustering analysis of C3d vs. T3d, C9d vs. T9d, and C15d vs. T15d (A–C) Statistical analysis of GO terms with significant enrichment and the top 30 GO terms in C3d vs. T3d, C9d vs. T9d, and C15d vs. T15d. The broken line graph shows the number of genes in the corresponding GO terms. (D–F) Heat map clustering analysis of plant defense response function entries differentially in C3d vs. T3d, C9d vs. T9d, and C15d vs. T15d. Note: The colors in the heatmap represent the normalized expression of the gene in each group.

with ID arahy.Tifrunner.gnm1.ann1.NH8LJ7 was up-regulated in C3d vs. T3d and C9d vs. T9d and down-regulated in C15d vs. T15d, and is a gene encoding MLP-like protein 43. The gene with the gene ID arahy.Tifrunner.gnm1.ann1.VFVG10 was up-regulated in C3d vs. T3d, C9d vs. T9d, and C15d vs. T15d and is a gene encoding the disease resistance protein (TIR-NBS-LRR class).

Analysis of the kyoto encyclopedia of genes and genomes enrichment pathway of differentially expressed genes in response to nematode treatment
 Statistical analysis of the DEGs in C3d vs. T3d, C9d vs. T9d, and C15d vs. T15d with significant enrichment in the top 20 KEGG pathways revealed that ubiquinone and other terpenoid-quinone biosynthesis pathway, plant hormone

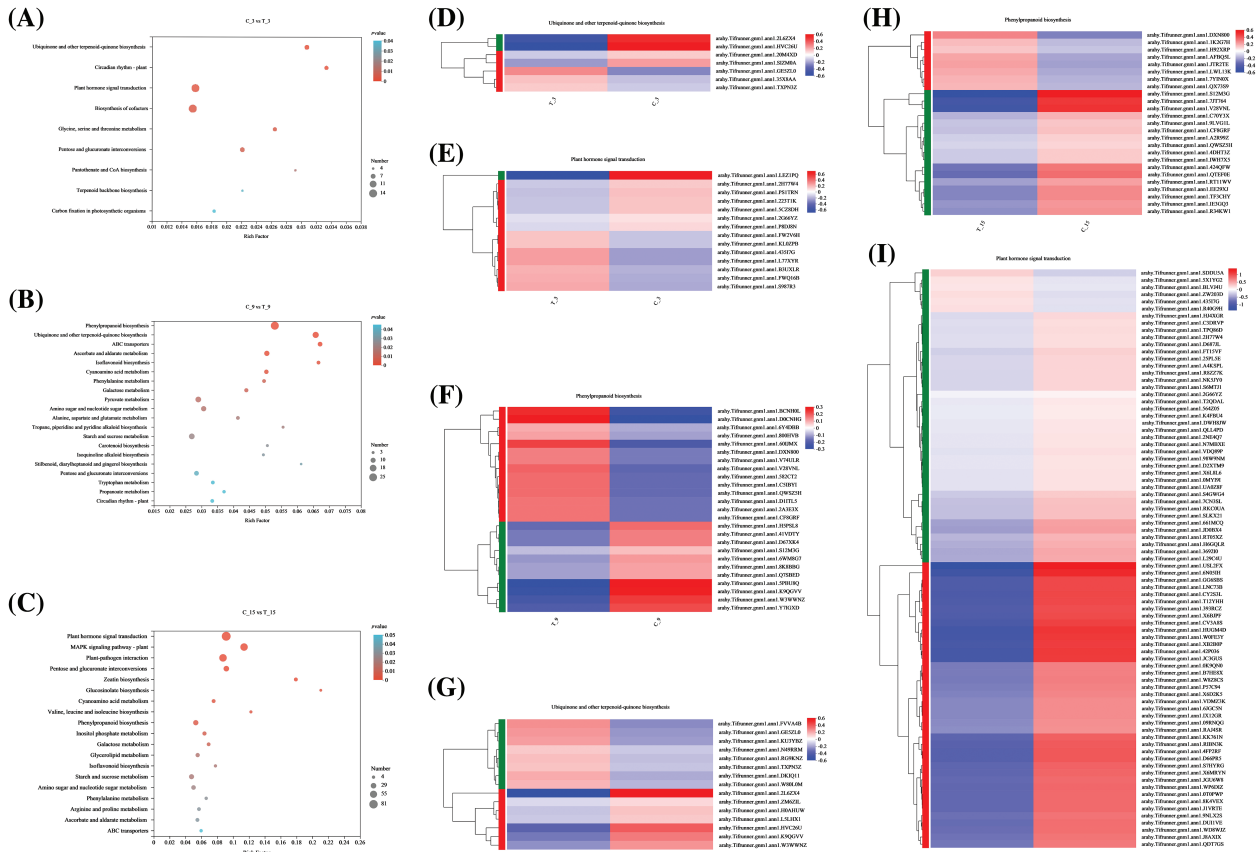


FIGURE 5. Kyoto Encyclopedia of Genes and Genomes (KEGG) pathway enrichment results and heat map clustering analysis. (A–C) Statistical analysis of KEGG pathway with significant enrichment and enrichment in the top 30 KEGG pathway in C3d vs. T3d, C9d vs. T9d, and C15d vs. T15d. Bubble size represents the number of genes with the difference. The color of the bubble represents the degree of significant enrichment. (D–I) Heat map clustering analysis of differential genes in ubiquinone and other terpenoid-quinone biosynthesis pathway, plant hormone signal transduction pathway, and phenylpropanoid biosynthesis pathway. Note: The colors in the heatmap represent the normalized expression of the gene in each group.

signal transduction pathway and phenylpropanoid biosynthesis pathway were associated with nematode treatment and more genes enrichments in these three pathways (Figs. 5A–5C).

In C3d vs. T3d, 7 DEGs were enriched in ubiquinone and other terpenoid-quinone biosynthesis pathway, wherein 3 were up-regulated and 4 were down-regulated (Fig. 5D), and 14 DEGs were enriched in plant hormone signal transduction pathway, wherein 7 were up-regulated, and 7 were down-regulated (Fig. 5E). Twenty-five genes in C9d vs. T9d were enriched in the phenylpropanoid biosynthesis pathway, of which 14 were up-regulated and 11 were down-regulated (Fig. 5F). Moreover, 15 genes were enriched in the ubiquinone and other terpenoid-quinone biosynthesis pathway, of which 8 were up-regulated and 7 were down-regulated (Fig. 5G). Twenty-five genes in C15d vs. T15d were enriched in the phenylpropanoid biosynthesis pathway, in which 8 were up-regulated and 17 were down-regulated (Fig. 5H). In the KEGG enrichment plots of C15d vs. T15d, the largest number of genes was enriched in the plant hormone signaling metabolic pathway. Eighty-one genes were enriched in the plant hormone signal transduction pathway, of which 6 genes were up-regulated and 75 were down-regulated (Fig. 5I). The results showed that the above-mentioned DEGS regulate the ubiquinone and other

terpenoid-quinone biosynthesis pathway, plant hormone signal transduction pathway, and phenylpropanoid biosynthesis pathway inside the *A. hypogaea* root by activating or inhibiting its own expression in response to the stress of nematodes.

Quantitative real-time PCR (qRT-PCR) analysis validation of differentially expressed genes

Statistical analysis of the changes of the genes number in ubiquinone and other terpenoid-quinone biosynthesis, plant hormone signal transduction, and phenylpropanoid biosynthesis KEGG pathway at 3, 9, and 15 d showed that the number of genes in ubiquinone and other terpenoid-quinone biosynthesis varied by 7, 15 and 5, respectively, with the prolongation of nematode treatment time. The number of genes annotated to the plant hormone signal transduction pathway with increased nematode treatment time was 14, 13, and 81, respectively. The number of genes annotated to the phenylpropanoid biosynthesis pathway with increased nematode treatment time was 5, 25, and 25, respectively (Fig. 6A). At the time limit set by this experiment, there were more DEGs in the early stage of nematode stress than in the later stage to regulate the ubiquinone and other terpenoid-quinone biosynthesis pathway. In the later stage of nematode stress, there were

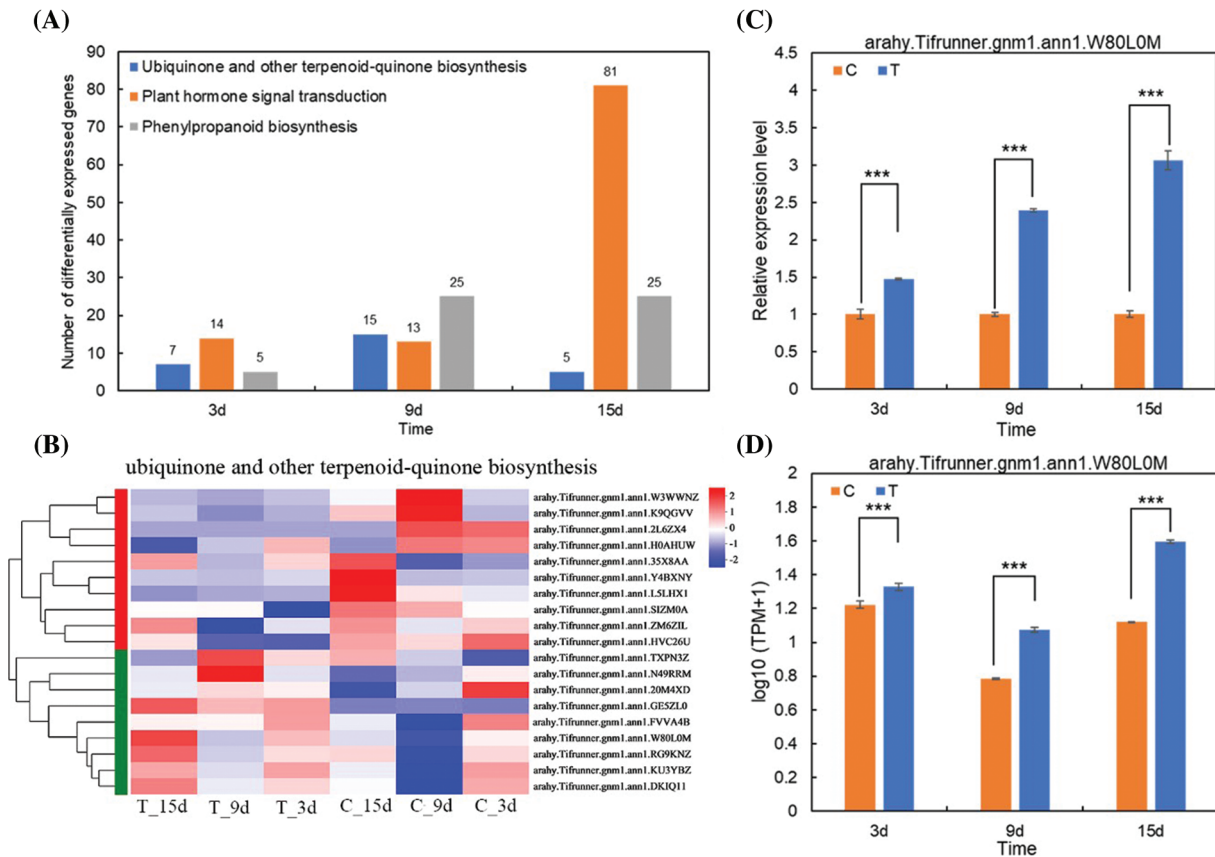


FIGURE 6. Analysis of target gene selection and validation. (A) Changes in the genes number in ubiquinone and other terpenoid-quinone biosynthesis, plant hormone signal transduction and phenylpropanoid biosynthesis Kyoto Encyclopedia of Genes and Genomes pathway at 3, 9, and 15 d. (B) Heat map clustering analysis of different genes of ubiquinone and other terpenoid-quinone biosynthesis pathway in each group. (C) Quantitative real-time PCR verification of target genes in 3, 9, and 15 d treatment groups and control groups. (D) Statistics of target gene RNA-Seq values in 3, 9, and 15 d treatment groups and control groups. Note: *** indicates extremely significant difference at 0.001 level.

more DEGs that regulate plant hormone signal transduction pathway and phenylpropanoid biosynthesis pathway.

Nineteen DEGs were enriched in the ubiquinone and other terpenoid-quinone biosynthesis pathway in the C3d vs. T3d, C9d vs. T9d, and C15d vs. T15d groups (Fig. 6B). Among these 19 genes, a significantly up-regulated gene in C3d vs. T3d, C9d vs. T9d, and C15d vs. T15d groups was selected (Table 3) to verify the accuracy of transcriptome sequencing analysis and provide reference to find target genes with positive effects on resistance to nematode stress. The verified gene was located on chromosome 8 of *A. hypogaea* and encodes homogentisate phytyltransferase (HPT). QRT-PCR results showed that the expression levels of the verified gene in the 3, 9, and 15 d treatment groups

were higher than that of the corresponding control groups (Fig. 6C). The expression trend of the gene verified by qRT-PCR was consistent with its transcriptome sequencing analysis (Fig. 6D), indicating that transcriptome sequencing data were accurate and reliable.

Discussion

Many studies have shown that the relationship between *A. hypogaea* and *M. incognita* is incompatible and interactive, but the resistance mechanism was unclear. A full understanding of the inhibiting effects of *A. hypogaea* will provide more ways for the biological control of *M. incognita*. In this study, the Pluronic F-127 system was used

TABLE 3

List of target gene in ubiquinone and other terpenoid-quinone biosynthesis pathway

KO ID	Gene ID	Regulation	p-value C3d VS T3d C9d VS T9d C15d VS T15d	Description	Location
K09833	arahy.Tifrunner.gnm1.ann1.W80L0M (<i>AhHPT</i>)	Up	1.7445E-54 0.0009 5.1065E-10	Homogentisate phytyltransferase 1	arahy.Tifrunner.gnm1.Arah08

to verify the tendency of the J2s to the excised root tips of *A. hypogaea* under visual conditions, similar to the phenomenon reported in studies (Wang *et al.*, 2009; Williamson and Čepulytė, 2017). The number of nematodes near the plant root tip is also different due to the different factors such as nematode species, number of inoculations, selected plant species, root tip length, and other factors in the system. The chemotactic migration rate of *M. incognita* J2s to the excised *A. hypogaea* root tips increased initially and then decreased along with the extension of observation; the staining result showed that the J2s of *M. incognita* could infect the *A. hypogaea* root tips. However, there were no knots at the surface of *A. hypogaea* roots inoculated with *M. incognita* J2s in the pot experiment, consistent with an earlier report (Vijayalakshni and Goswami, 1987). These phenomena indicated that *A. hypogaea* may be a trap plant capable of attracting and inducing *M. incognita* J2s infestation, while further development and propagation of *M. incognita* were inhibited in *A. hypogaea* root system (Waisen *et al.*, 2019; Sacchi *et al.*, 2021). The environment of the *A. hypogaea* root system is not conducive to the survival and breeding of *M. incognita* (Bendezu and Starr, 2003).

High-throughput sequencing technology, with its advantages of high sensitivity, high accuracy and low cost, has been gradually applied by many scholars in the study of species and diseases (Sapkota and Nicolaisen, 2015; Yang *et al.*, 2016). In this study, statistical analysis was conducted to find the DEGs after *M. incognita* J2s infestation.

Through transcriptome sequencing of 6 groups (18 samples), the Q30 (%) value of sequence data after quality control was more than 93.71%, and the matching rate of reference gene was more than 95.73%, indicating the accuracy and reliability of sequencing results. The number of significant DEGs in C3d vs. T3d, C9d vs. T9d, and C15d vs. T15d was counted by transcriptomic sequencing based on RNA-seq, and the number of genes with significant differential expression increased with the increase in the number of stress days. After 7, 14, and 28 days of infestation by *M. incognita*, the DEG numbers in the eggplant (*Solanum melongena* L.) also increased (Zhang *et al.*, 2021), but the DEGs numbers in the rice (*Oryza sativa* L.) root system after 6 days of *M. incognita* infestation was higher than that after 18 days (Zhou *et al.*, 2020). Dicotyledonous plants and monocotyledonous plants have some differences in the infection response to root-knot nematode (Przybylska and Obrepalska-Stęplowska, 2020).

GO functional enrichment analysis of the three groups of DEGs showed that the DEGs in each group were enriched in the GO term of plant defense response, and one gene encoding defense protein (TIR-NBS-LRR class) was found in all three groups. The invasion of plant pathogens triggers the immune defense system, in which the second defense layer (ETI) in plants is mediated by the plant resistance gene (*R* gene) (Meyers *et al.*, 1999). Most *R* genes have been found in plants with nucleotide binding sites (NBS) and leucine-rich repeat (LRR) domains. A subfamily of NBS-LRR proteins and TIR-NBS-LRR proteins with a Toll/interleukin-1 receptor domain at the N-terminus have been found in *Arabidopsis* (*Arabidopsis thaliana* L.) (Botella *et al.*, 1998),

soybean (*Glycine max* L.) (Li *et al.*, 2022), chickpea (*Cicer arietinum* L.) (Sagi *et al.*, 2017) and other plants and are associated with plant disease resistance.

KEGG pathway enrichment analysis of the three groups of DEGs showed that ubiquinone and other terpenoid-quinone biosynthesis, plant hormone signal transduction, and phenylpropanoid biosynthesis were the main metabolic pathways in *A. hypogaea* responding to *M. incognita* stress. The candidate gene selected from the ubiquinone and other terpenoid-quinone biosynthesis pathway encodes HPT, the key rate-limiting enzyme for the synthesis of α -tocopherol (Hunter and Cahoon, 2007; Kurmaz *et al.*, 2022). The HPT super-expressing plants had significantly increased content of α -tocopherol (Crowell *et al.*, 2008). In addition, the silencing of the *HPT* gene in tobacco by dsRNAi technology reduced the content of tocopherol in tobacco and increased the sensitivity of plants to abiotic stress compared with wild-type plants (Abbasi *et al.*, 2007). At present, many studies have found that α -tocopherol plays a positive role in plant growth under the stress of abiotic factors such as low temperature (Maeda *et al.*, 2006), drought (Liu *et al.*, 2008), high salt (Abbasi *et al.*, 2007), and heavy metal ions (Collin *et al.*, 2008). Tocopherol has antioxidant effects, which can remove oxygen free radicals to affect the growth and development of parasites (Apel and Hirt, 2004; Taylor *et al.*, 1997; Ibrahim *et al.*, 2012). In addition, α -tocopherol can slow down plant damage and aging (Austin *et al.*, 2006; Sattler *et al.*, 2006; Abbasi *et al.*, 2009). α -Tocopherol is also involved in the transduction of cell signals in plants, and studies have shown that hormone levels in plants, such as jasmonic acid and ethylene, are related to the synthesis and regulation of tocopherol. In fact, plant hormones have been shown to play a key role in coordinating the signal response to nematode infection (Falk *et al.*, 2002; Cela *et al.*, 2009; Singh *et al.*, 2011). The treatment of soybeans with methyl jasmonate and sodium nitroprusside could improve the resistance of soybeans to *Spodoptera littoralis*, and α -tocopherol detection was performed on treated soybeans, both of which were significantly increased (Mohamed *et al.*, 2021). Therefore, we suggest that there is a correlation between the *AhHPT* gene and α -tocopherol expression, which further plays a key role in the resistance of *A. hypogaea* against *M. incognita*. The results indicated that the *AhHPT* gene may be an active regulatory gene that can be applied to plant molecular breeding with resistance against *M. incognita*.

Conclusion

The excised root tips of *A. hypogaea* had a certain attraction effect on *M. incognita* J2s, which could invade the excised and intravital *A. hypogaea* root. The DEGs of C3d vs. T3d, C9d vs. T9d, and C15d vs. T15d were 462,1057 and 2099, respectively. These DEGs were mainly related to plant defense response function and were enriched in ubiquinone and other terpenoid-quinone biosynthesis, plant hormone signal transduction, and phenylpropanoid biosynthesis pathways. The candidate gene *AhHPT* was identified in ubiquinone and other terpenoid-quinone biosynthesis

pathway, which may be involved in the regulation of *A. hypogaea* resistance to *M. incognita*.

Acknowledgement: None.

Funding Statement: This work was supported by the Post-Doctoral Program of Hebei Province (2019003011) and Foundation of President of Hebei University (XZJJ201924).

Author Contributions: The authors confirm contribution to the paper as follows: study conception and design: Jianfeng Liu and Dandan Cao; data collection: Yuanyuan Zhou and Jianqing Ma; analysis and interpretation of results: Xinyi Peng and Xiaohong Fu; draft manuscript preparation: Xuejin Yang. All authors reviewed the results and approved the final version of the manuscript.

Availability of Data and Materials: The datasets generated during and/or analyzed during the current study are available from the corresponding author upon reasonable request.

Ethics Approval: Not applicable.

Conflicts of Interest: The authors declare that they have no conflicts of interest to report regarding the present study.

References

- Abad P, Gouzy J, Aury J, Castagnone-Sereno P, Danchin EG et al. (2008). Genome sequence of the metazoan plant-parasitic nematode *Meloidogyne incognita*. *Nature Biotechnology* **26**: 909–915. <https://doi.org/10.1038/nbt.1482>
- Abbasi AR, Hajirezaei M, Hofius D, Sonnewald U, Voll LM (2007). Specific roles of α - and γ -tocopherol in abiotic stress responses of transgenic tobacco. *Plant Physiology* **143**: 1720–1738. <https://doi.org/10.1104/pp.106.094771>
- Abbasi AR, Saur A, Hennig P, Tschiersch H, Hajirezaei M, Hofius D, Sonnewald U, Voll LM (2009). Tocopherol deficiency in transgenic tobacco (*Nicotiana tabacum* L.) plants leads to accelerated senescence. *Plant Cell Environment* **32**: 144–157. <https://doi.org/10.1111/j.1365-3040.2008.01907.x>
- Aioub AA, Elesawy AE, Ammar EE (2022). Plant growth promoting rhizobacteria (PGPR) and their role in plant-parasitic nematodes control: A fresh look at an old issue. *Journal of Plant Diseases and Protection* **129**: 1305–1321. <https://doi.org/10.1007/s41348-022-00642-3>
- Ali AA, EI-Ashry RM, Aioub AAA (2022). Animal manure rhizobacteria co-fertilization suppresses phytonematodes and enhances plant production: Evidence from field and greenhouse. *Journal of Plant Diseases and Protection* **129**: 155–169. <https://doi.org/10.1007/s41348-021-00529-9>
- Apel K, Hirt H (2004). Reactive oxygen species: Metabolism, oxidative stress, and signal transduction. *Annual Review of Plant Biology* **55**: 373–399. <https://doi.org/10.1146/annurev.arplant.55.031903.141701>
- Austin JN, Frost E, Vidi PA, Kessler F, Staehelin LA (2006). Plastoglobules are lipoprotein subcompartments of the chloroplast that are permanently coupled to thylakoid membranes and contain biosynthetic enzymes. *Plant Cell* **18**: 169–1703. <https://doi.org/10.1105/tpc.105.039859>
- Belcher JV, Hussey RS (1977). Influence of *Tagetes patula* and *Arachis hypogaea* on *Meloidogyne incognita*. *Plant Disease Reporter* **61**: 525–528.
- Bendezu IF, Starr JL (2003). Mechanism of resistance to *Meloidogyne arenaria* in the peanut cultivar COAN. *Journal of Nematology* **35**: 115–118.
- Botella MA, Parker JE, Frost LN, Bittner-Eddy PD, Beynon JL, Daniels MJ, Holub EB, Jones JD (1998). Three genes of the Arabidopsis *RPP1* complex resistance locus recognize distinct *Peronospora parasitica* avirulence determinants. *The Plant Cell* **10**: 1847–1860. <https://doi.org/10.1105/tpc.10.11.1847>
- Byrd DW, Kirkpatrick T, Barker KR (1983). An improved technique for clearing and staining plant tissue for detection of nematodes. *Journal of Nematology* **15**: 142–143.
- Cela J, Falk J, Munné-Bosch S (2009). Ethylene signaling may be involved in the regulation of tocopherol biosynthesis in *Arabidopsis thaliana*. *FEBS Letters* **583**: 992–996. <https://doi.org/10.1016/j.febslet.2009.02.036>
- Çiftçi S, Suna G (2022). Functional components of peanuts (*Arachis hypogaea* L.) and health benefits: A review. *Future Foods* **5**: 100140.
- Collin VC, Eymery F, Genty B, Rey P, Havaux M (2008). Vitamin E is essential for the tolerance of *Arabidopsis thaliana* to metal-induced oxidative stress. *Plant Cell and Environment* **31**: 244–257. <https://doi.org/10.1111/j.1365-3040.2007.01755.x>
- Crowell EF, McGrath JM, Douches DS (2008). Accumulation of vitamin E in potato (*Solanum tuberosum*) tubers. *Transgenic Research* **17**: 205–217. <https://doi.org/10.1007/s11248-007-9091-1>
- Davis EL, Baum TJ, Bakker J, Schots A, Hussey RS (2000). Nematode parasitism genes. *Annual Review of Phytopathology* **38**: 365–396.
- Dong WB, Holbrook CC, Timper P, Brenneman TB, Chu Y, Ozias-Akins P (2008). Resistance in peanut cultivars and breeding lines to three root-knot nematode species. *Plant Disease* **92**: 631–638. <https://doi.org/10.1094/PDIS-92-4-0631>
- Du C, Jiang J, Zhang H, Zhao T, Yang H, Zhang D, Zhao Z, Xu X, Li J (2020). Transcriptomic profiling of *Solanum peruvianum* LA3858 revealed a *Mi-3*-mediated hypersensitive response to *Meloidogyne incognita*. *BMC Genomics* **21**: 250. <https://doi.org/10.1186/s12864-020-6654-5>
- EI-Ashry RM, Aioub AAA, Awad SE (2023). Suppression of *Meloidogyne incognita* (Tylenchida: Heteroderidae) and *Tylenchulus semipenterans* (Tylenchida: Tylenchulidae) using *Tilapia* fish powder and plant growth promoting rhizobacteria *in vivo* and *in vitro*. *European Journal of Plant Pathology* **165**: 665–676. <https://doi.org/10.1007/s10658-023-02637-8>
- El-Sappah AH, Islam MM, El-awady HH, Yan S, Qi S, Liu J, Cheng G, Liang Y (2019). Tomato natural resistance genes in controlling the root-knot nematode. *Genes* **10**: 925. <https://doi.org/10.3390/genes10110925>
- Eldeeb AM, Farag AAG, AI-Harbi MS, Kesba H, Sayed S, Elesawy AE, Hendawi MA, Mostafa EM, Aioub AAA (2022). Controlling of *Meloidogyne incognita* (Tylenchida: Heteroderidae) using nematicides, *Linum usitatissimum* extract and certain organic acids on four peppers cultivars under greenhouse conditions. *Saudi Journal of Biological Sciences* **29**: 3107–3113. <https://doi.org/10.1016/j.sjbs.2022.03.018>

- Elnahal ASM, El-Saadony MT, Saad AM, Desoky EM, El-Tahan AM, Rady MM, AbuQamar SF, El-Tarabily KA (2022). The use of microbial inoculants for biological control, plant growth promotion, and sustainable agriculture: A review. *European Journal of Plant Pathology* **162**: 759–792. <https://doi.org/10.1007/s10658-021-02393-7>
- Falk J, Krauß N, Dähnhardt D, Krupinska K (2002). The senescence associated gene of barley encoding 4-hydroxyphenylpyruvate dioxygenase is expressed during oxidative stress. *Journal of Plant Physiology* **159**: 1245–1253. <https://doi.org/10.1078/0176-1617-00804>
- Faske TR, Starr JL (2009). Reproduction of *Meloidogyne marylandi* and *M. incognita* on several Poaceae. *Journal of Nematology* **41**: 2–4.
- Hunter SC, Cahoon EB (2007). Enhancing vitamin E in oilseeds: Unraveling tocopherol and tocotrienol biosynthesis. *Lipids* **42**: 97–108. <https://doi.org/10.1007/s11745-007-3028-6>
- Ibrahim HM, Hosseini P, Alkharouf NW, Hussein EH, El-Din AE, Aly MA, Matthews BF (2011). Analysis of gene expression in soybean (*Glycine max*) roots in response to the root knot nematode *Meloidogyne incognita* using microarrays and KEGG pathways. *BMC Genomics* **12**: 220. <https://doi.org/10.1186/1471-2164-12-220>
- Ibrahim MA, Zuwahu MM, Isah MB, Jatau ID, Aliyu AB, Umar IA (2012). Effects of vitamin E administration on *Plasmodium berghei* induced pathological changes and oxidative stress in mice. *Tropical Biomedicine* **29**: 98–106.
- Jaouannet M, Perfus-Barbeoch L, Deleury E, Magliano M, Engler G et al. (2012). A root-knot nematode-secreted protein is injected into giant cells and targeted to the nuclei. *The New phytologist* **194**: 924–931. <https://doi.org/10.1111/j.1469-8137.2012.04164.x>
- Johnson AW, Dowler CC, Handoo ZA (2000). Population dynamics of *Meloidogyne incognita*, *M. arenaria*, and other nematodes and crop yields in rotations of cotton, peanut, and wheat under minimum tillage. *Journal of Nematology* **32**: 52–61.
- Johnson AW, Minton NA, Brenneman TB, Todd JW, Herzog GA, Gascho GJ, Baker SH, Bondari Y (1998). Peanut-cotton-rye rotations and soil chemical treatment for managing nematodes and thrips. *Journal of Nematology* **30**: 211–225.
- Jones JT, Haegeman A, Danchin EG, Gaur HS, Helder J et al. (2013). Top 10 plant-parasitic nematodes in molecular plant pathology. *Molecular Plant Pathology* **14**: 946–961. <https://doi.org/10.1111/mp.12057>
- Kim D, Langmead B, Salzberg SL (2015). HISAT: A fast spliced aligner with low memory requirements. *Nature methods* **12**: 357–360. <https://doi.org/10.1038/nmeth.3317>
- Kurmaz SV, Fadeeva NV, Skripets JA, Komendant RI, Ignatiev VM, Emel'yanova NS, Soldatova YV, Faingold II, Poletaeva DA, Kotelnikova RA (2022). New water-soluble forms of a-tocopherol: Preparation and study of antioxidant activity *in vitro*. *Mendeleev Communications* **32**: 117–119. <https://doi.org/10.1016/j.mencom.2022.01.038>
- Li B, Dewey CN (2011). RSEM: Accurate transcript quantification from RNA-Seq data with or without a reference genome. *BMC Bioinformatics* **12**: 323. <https://doi.org/10.1186/1471-2105-12-323>
- Li Z, Deng S, Xuan H, Fan X, Sun R, Zhao J, Wang H, Guo N, Xing H (2022). A novel TIR-NBS-LRR gene regulates immune response to Phytophthora root rot in soybean. *The Crops Journal* **10**: 1644–1653. <https://doi.org/10.1016/j.cj.2022.03.003>
- Liu X, Hua X, Guo J, Qi D, Wang L, Liu Z, Jin Z, Chen S, Liu G (2008). Enhanced tolerance to drought stress in transgenic tobacco plants overexpressing *VTE1* for increased tocopherol production from *Arabidopsis thaliana*. *Biotechnology Letters* **30**: 1275–1280.
- Love MI, Huber W, Anders S (2014). Moderated estimation of fold change and dispersion for RNA-seq data with DESeq2. *Genome Biology* **15**: 550. <https://doi.org/10.1186/s13059-014-0550-8>
- Maeda H, Song W, Sage TL, DellaPenna D (2006). Tocopherols play a crucial role in low-temperature adaptation and phloem loading in *Arabidopsis*. *Plant Cell* **18**: 2710–2732. <https://doi.org/10.1105/tpc.105.039404>
- Mao Z, Zhu P, Liu F, Huang Y, Ling J, Chen G, Yang Y, Feng D, Xie B (2015). Cloning and functional analyses of pepper *CaRKNR* involved in *Meloidogyne incognita* resistance. *Euphytica* **205**: 903–913. <https://doi.org/10.1007/s10681-015-1438-8>
- Meyers BC, Dickerman AW, Micheltmore RW, Sivaramakrishnan S, Sobral BW, Young ND (1999). Plant disease resistance genes encode members of an ancient and diverse protein family within the nucleotide-binding superfamily. *Plant Journal* **20**: 317–332. <https://doi.org/10.1046/j.1365-313x.1999.t01-1-00606.x>
- Moens M, Perry RN, Starr JL (2009). *Meloidogyne Species: A Diverse Group of Novel and Important Plant Parasites*, pp. 1–17. Wallingford, UK: CABI Publishing.
- Mohamed HI, Mohammed AH, Mohamed NM, Ashry NA, Zaky LM, Mogazy AM (2021). Comparative effectiveness of potential elicitors of soybean plant resistance against *Spodoptera littoralis* and their effects on secondary metabolites and antioxidant defense system. *Gesunde Pflanzen* **73**: 273–285. <https://doi.org/10.1007/s10343-021-00546-6>
- Nishat Y, Danish M, Mohamed HI, Shaikh H, Elhakem A (2022). Biological control of root-knot nematode *Meloidogyne incognita* in *Psoralea corylifolia* plant by enhancing the biocontrol efficacy of *Trichoderma harzianum* using Press Mud. *Phyton-International Journal of Experimental Botany* **91**: 1757–1777. <https://doi.org/10.32604/phyton.2022.021267>
- Oka YJ, Koltai H, Bar-Eyal M, Mor M, Sharon E, Chet I, Spiegel Y (2015). New strategies for the control of plant-parasitic nematodes. *Pest Management Science* **56**: 983–988. [https://doi.org/10.1002/1526-4998\(200011\)56:11<983::aid-ps233>3.0.co;2-x](https://doi.org/10.1002/1526-4998(200011)56:11<983::aid-ps233>3.0.co;2-x)
- Pertea M, Pertea GM, Antonescu CM, Chang TC, Mendell J, Salzberg SL (2015). StringTie enables improved reconstruction of a transcriptome from RNA-seq reads. *Nature Biotechnology* **33**: 290–295. <https://doi.org/10.1038/nbt.3122>
- Przybylska A, Obrępańska-Stęplowska A (2020). Plant defense responses in monocotyledonous and dicotyledonous host plants during root-knot nematode infection. *Plant and Soil* **451**: 239–260. <https://doi.org/10.1007/s11104-020-04533-0>
- Reynolds AM, Dutta TK, Curtis RH, Powers SJ, Gaur HS, Kerry BR (2015). Chemotaxis can take plant-parasitic nematodes to the source of a chemo-attractant via the shortest possible routes. *Journal of the Royal Society Interface* **8**: 568–577. <https://doi.org/10.1098/rsif.2010.0417>
- Sacchi S, Torrini G, Marianelli L, Mazza G, Fumagalli A, Cavagna B, Ciampitti M, Roversi PF (2021). Control of *Meloidogyne graminicola* a root-knot nematode using rice plants as trap crops: Preliminary results. *Agriculture* **11**: 37. <https://doi.org/10.3390/agriculture11010037>

- Sagi MS, Deokar AA, Tar'an B (2017). Genetic analysis of NBS-LRR gene family in chickpea and their expression profiles in response to *Ascochyta* blight infection. *Frontiers in Plant Science* **8**: 838. <https://doi.org/10.3389/fpls.2017.00838>
- Sapkota R, Nicolaisen M (2015). High-throughput sequencing of nematode communities from total soil DNA extractions. *BMC Ecology* **15**: 3. <https://doi.org/10.1186/s12898-014-0034-4>
- Sattler SE, Mène-Saffrané L, Farmer EE, Krischke M, Mueller MJ, DellaPenna D (2006). Nonenzymatic lipid peroxidation reprograms gene expression and activates defense markers in *Arabidopsis* tocopherol-deficient mutants. *Plant Cell* **18**: 3706–3720. <https://doi.org/10.1105/tpc.106.044065>
- Singh KB, Jayaswal P, Chandra S, Jayanthi M, Mandal PK (2022). Comparative transcriptome profiling of *Polianthes tuberosa* during a compatible interaction with root-knot nematode *Meloidogyne incognita*. *Molecular Biology Reports* **49**: 4503–4516. <https://doi.org/10.1007/s11033-022-07294-4>
- Singh RK, Ali SA, Nath P, Sane VA (2011). Activation of ethylene-responsive P-hydroxyphenylpyruvate dioxygenase leads to increased tocopherol levels during ripening in mango. *Journal of Experimental Botany* **62**: 3375–3385. <https://doi.org/10.1093/jxb/err006>
- Taylor DW, Levander OA, Krishna VR, Evans CB, Morris VC, Barta JR (1997). Vitamin E-efficient diets enriched with fish oil suppress lethal *Plasmodium yoelii* infections in athymic and scid/bg mice. *Infection and Immunity* **65**: 197–202. <https://doi.org/10.1128/iai.65.1.197-202.1997>
- Vijayalakshni K, Goswami BK (1987). Effect of root dip treatment of tomato seedlings of aqueous extracts of some oil-seed cakes on root-knot nematode infestation. *Annals of Agricultural Research* **8**: 168–171.
- Waisen P, Sipes BS, Wang KH (2019). Potential of biofumigant cover crops as open-end trap crops against root-knot and reniform nematodes. *Nematropica* **49**: 254–264.
- Wang C, Lower S, Williamson VM (2009). Application of Pluronic gel to the study of root-knot nematode behaviour. *Nematology* **11**: 453–464. <https://doi.org/10.1163/156854109x447024>
- Williamson VM, Čepulytė R (2017). Assessing attraction of nematodes to host roots using Pluronic gel medium. *Methods in Molecular Biology* **1573**: 261–268. https://doi.org/10.1007/978-1-4939-6854-1_19
- Wubben MJ, Callahan FE, Hayes RW, Jenkins JN (2008). Molecular characterization and temporal expression analyses indicate that the *MIC* (*Meloidogyne Induced Cotton*) gene family represents a novel group of root-specific defense-related genes in upland cotton (*Gossypium hirsutum* L.). *Planta* **228**: 111–123. <https://doi.org/10.1007/s00425-008-0723-3>
- Xie C, Mao X, Huang J, Ding Y, Wu J, Dong S, Kong L, Gao G, Li C, Wei L (2011). KOBAS 2.0: A web server for annotation and identification of enriched pathways and diseases. *Nucleic Acids Research* **39**: W316–W322. <https://doi.org/10.1093/nar/gkr483>
- Yang MX, Wang QX, Xiao H, Yang C (2016). Sequencing complete mitochondrial genome of *Lanius sphenocercus sphenocercus* (Passeriformes: Laniidae) using Illumina HiSeq 2500. *Mitochondrial DNA Part B-Resources* **1**: 306–307. <https://doi.org/10.1080/23802359.2016.1167640>
- Zhang M, Zhang H, Tan J, Huang S, Chen X, Jiang D, Xiao X (2021). Transcriptome analysis of eggplant root in response to root-knot nematode infection. *Pathogens* **10**: 470. <https://doi.org/10.3390/pathogens10040470>
- Zhou Y, Zhao D, Shuang L, Xiao D, Xuan Y et al. (2020). Transcriptome analysis of rice roots in response to root-knot nematode infection. *International Journal of Molecular Sciences* **21**: 848. <https://doi.org/10.3390/ijms21030848>